

ORIGINAL ARTICLE

Overcoming chemoresistance of non-small cell lung carcinoma through restoration of an AIF-dependent apoptotic pathwayM-A Gallego^{1,5}, C Ballot^{1,5}, J Kluza¹, N Hajji², A Martoriat¹, L Castéra¹, C Cuevas³, P Formstecher¹, B Joseph², G Kroemer⁴, C Bailly^{1,6} and P Marchetti¹¹INSERM U 837, Université Lille 2, Faculté de Médecine, Jean-Pierre Aubert Research Centre, Place de Verdun, Lille, France;²Institute of Environmental Medicine Karolinska Institutet, Stockholm, Sweden; ³PharmaMar, Avda. de los Reyes, 1,P.I. La Mina-Norte, E-28770 Colmenar Viejo, Madrid, Spain and ⁴INSERM U848, Institut Gustave Roussy, Villejuif, France

Non-small cell lung carcinomas (NSCLCs) are typically resistant against apoptosis induced by standard chemotherapy. We evaluated the effects of the two potential antitumor agents of the lamellarin class on a highly apoptosis-resistant NSCLC cell line. Both the marine alkaloid lamellarin-D and its synthetic amino derivative PM031379 induced the activation of Bax, the mitochondrial release of cytochrome *c* and apoptosis-inducing factor (AIF), as well as the activation of caspase-3. However, only PM031379 triggered cell death and sign of nuclear apoptosis coupled to the nuclear translocation of AIF. Depletion of AIF with small interfering RNA or microinjection of a neutralizing anti-AIF antibody largely prevented PM031379-induced cytotoxicity, underscoring the essential contribution of AIF to NSCLC killing. Using NSCLC cells lacking mitochondrial DNA, we showed that the generation of mitochondrial reactive oxygen species (ROS) was crucial for the PM031379-induced translocation of AIF to the nucleus and subsequently cell death. Pretreatment of NSCLC cells with menadione, a mitochondrial ROS generator, was able to restore the deficient chemotherapy-induced apoptosis of NSCLC cells. Altogether, these data suggest that mitochondrial ROS generation is crucial for overriding the chemoresistance of NSCLC cells. Moreover, this study delineates the unique mechanism of action of lamellarins as potential anticancer agents.

Oncogene (2008) 27, 1981–1992; doi:10.1038/sj.onc.1210833; published online 1 October 2007

Keywords: apoptosis; mitochondria; chemotherapy

Introduction

Chemotherapy resistance represents a major problem for the treatment of patients with lung carcinomas. Among these resistance mechanisms, defects in the cell death machinery are supposed to play an important role (Zhivotovsky and Orrenius, 2003). Indeed, molecular modifications hindering programmed cell death such as increased expression of anti-apoptotic genes and/or mutations in the intrinsic apoptotic pathway participate in the resistance to anticancer treatment (Johnstone *et al.*, 2002). We previously demonstrated that the resistance of non-small cell lung carcinomas (NSCLCs) cells to conventional cytotoxic drugs can be explained by a defect that affects the post-mitochondrial phase of the apoptotic process (Joseph *et al.*, 2001; Gallego *et al.*, 2004). Despite this knowledge, a better understanding of signaling pathways in resistant cells is needed to overcome resistance and to reactivate their sensitivity to anticancer treatment.

Mitochondria are at the crossroads of apoptotic pathways induced by anticancer agents, at several levels. In response to apoptotic stimuli, the outer mitochondrial membrane is permeabilized, causing the release of proteins from the mitochondrial intermembrane space. Several intermembrane space proteins, notably cytochrome *c* (Cyt *c*) can trigger the activation of caspases. Other intermembrane space proteins can trigger caspase-independent apoptotic events. One of the most prominent caspase-independent death effector released from intermembrane space is apoptosis-inducing factor (AIF). To become fully effective as an apoptosis inducer, AIF is first released from mitochondria and then imported into the nucleus to induce chromatin condensation and DNA degradation (Galluzzi *et al.*, 2006). The action of AIF is critical for cell death induction by some anticancer agents. Thus, the depletion of AIF with small interfering RNAs (siRNAs) or the neutralization of AIF with micro-injected antibodies can inhibit the death of (i) neuroblastoma (Gabellini *et al.*, 2006), (ii) NSCLC cells responding to tyrosine kinase inhibitors (Gallego *et al.*, 2004), (iii) colon cancer cells responding to the non-steroidal anti-inflammatory drug sulindac (Park *et al.*, 2005b), (iv) cervical cancer cells treated with arsenic trioxide (Kang *et al.*, 2004b),

Correspondence: Professor P Marchetti, INSERM U 837, 1 Place de Verdun, Lille Cedex F-59045, France.

E-mail: philippe.marchetti@lille.inserm.fr

⁵These authors contributed equally to this work

⁶Current address: Institut de Recherche Pierre Fabre, 3 rue des satellites, 31432 Toulouse, France.

Received 11 May 2007; revised 12 July 2007; accepted 31 August 2007; published online 1 October 2007

(v) leukemia cells subjected to photodynamic therapy (Furre *et al.*, 2005) and (vi) prostate cancer cells exposed to titanocene drugs (O'Connor *et al.*, 2006). Furthermore, in highly resistant NSCLC cells where the caspase-dependent pathway is defective, activation of a caspase-independent, AIF-mediated mitochondrial signaling pathway restores NSCLC cell death (Gallego *et al.*, 2004) substantiating the importance of alternative (caspase-independent) mechanisms for effective cancer therapy. Likewise, it is worth noting that the resistance to radiation can be reversed through activation of nuclear translocation of AIF (Park *et al.*, 2005a).

In addition to the release of catabolic enzymes (or activator of such enzymes), mitochondria can contribute to cell death by affecting redox and bioenergetic equilibria. A variety of anticancer drugs trigger mitochondria to generate reactive oxygen species (ROS) that contribute to apoptotic signaling (Engel and Evens 2006). The apoptosis-associated ROS generation results from a dysfunction of the mitochondrial respiratory chain and/or an increase in mitochondrial membrane permeability. Elevated levels of ROS contribute to the cellular oxidation observed in late apoptosis. Then, ROS serve as intracellular second messengers that modulate the activation of numerous signaling pathways and/or the expression of pro-apoptotic genes. Moreover, ROS generation can also favor the mitochondrial permeability increase in a self-amplifying loop that contributes to locking the cell into an irreversible commitment to death.

An over-growing body of evidence indicates that mitochondria, by virtue of their prominent role in apoptosis, constitute a potential pharmacological target for new antitumor drugs. We recently discovered that this applies for the marine alkaloid lamellarin-D (Lam-D) and its synthetic amino derivative PM031379 (Kluza *et al.*, 2006). Both Lam-D and PM031379 induce mitochondria isolated from leukemia cells to swell and to release apoptogenic effectors that provoke nuclear apoptosis (Kluza *et al.*, 2006). Lam-D functions also as a potent topoisomerase I poison (Facompre *et al.*, 2003).

The aim of this study was to achieve a better understanding of apoptotic signaling in NSCLC focusing on mitochondrion-related events. To this end, we used two prototypic lamellarins Lam-D and PM031379 as pharmacological tools to decipher the apoptotic networks in the chemoresistant NSCLC cell line U1810. Our data reveal that mitochondrial ROS play a major role in determining the susceptibility to cell death, presumably by modulating the nuclear translocation of AIF.

Results

PM031379, but not Lam-D, induces nuclear apoptosis in NSCLC cells

From a structural point of view, Lam-D and PM031379 only differ by the nature of the substituent linked to the central pyrrole ring of the common planar pentacyclic chromophore. As shown in Figure 1a, Lam-D bears a

methoxy-phenol moiety, whereas PM031379 displays an aminopropine side chain. We have shown previously that both agents are equipotent cell death inducers when added to leukemia cells (Kluza *et al.*, 2006). However, the two molecules exhibited a major difference in their cytotoxic potential when added to the highly chemoresistant NSCLC cell line U1810 (Gallego *et al.*, 2004). After 18 h of incubation, a marked dose-dependent increase in nuclear apoptosis was observed with PM031379 as documented by the appearance of a sub-G1 peak (Figure 1b, left panel), along with oligonucleosomal DNA fragmentation (Figure 1c). Kinetic experiments (from 1 to 24 h) revealed a significant increase in nuclear apoptosis that was detected by 12 h after incubation with 10 μ M PM031379 (Figure 1b, right panel). U1810 cells treated with PM031379 manifested the morphological hallmarks of apoptosis, namely chromatin and cytoplasmic condensation, as well as nuclear fragmentation (Figure 1d). In strict contrast to PM031379, Lam-D failed to induce subdiploidy (Figure 1b) DNA fragmentation (Figure 1c) or other features of apoptosis (Figure 1d) in U1810 cells. Similar results were obtained in the NSCLC cell line, A549 (Figure 1e). These results suggest that Lam-D and its derivative PM031379 markedly differ in their ability to trigger the apoptotic cascade in NSCLC cells.

Apoptotic cascade triggered by Lam-D and PM031379 in NSCLC cells

We have previously reported that Lam-D and PM031379 triggered mitochondrion-dependent apoptosis (Kluza *et al.*, 2006). To define the apoptotic cascade induced by PM031379 in NSCLC cells and also in that way the mechanisms of resistance to Lam-D, we focused on two major events contributing to nuclear apoptosis, namely the mitochondrial release of the pro-apoptotic factors AIF and Cyt *c* and the activation of effector caspases (Figure 2). Because Bax is a prominent mediator of the outer mitochondrial membrane permeabilization in apoptosis, we first examined whether PM031379 was capable of activating Bax in U1810 cells (Figure 2a). Using the 6A7 antibody, which only recognizes the membrane-bound active form of Bax, we showed that PM031379 lead to significant Bax activation, as detectable by immunofluorescence staining followed by cytofluorometric analysis (Figure 2a, upper panel) or immunofluorescence microscopy (Figure 2a, lower panel). PM031379-treated cells showed a punctuate, cytoplasmic staining pattern of activated Bax, consistent with a mitochondrial localization of Bax. This contrasts with the diffuse, presumably cytosolic staining pattern of Bax found in control cells. As expected from its effect on Bax activation, PM031379 induced the relocation of two major pro-apoptotic factors, Cyt *c* and AIF, from mitochondria to the cytosol, as determined by immunoblotting (Figure 2b). Significant induction of a caspase-3/7-like enzymatic activity was detected in PM031379-treated U1810 cells (Figure 2c). Unexpectedly, we also observed that Lam-D, like PM031379, induced Bax activation (Figure 2a) and AIF release to the cytosol

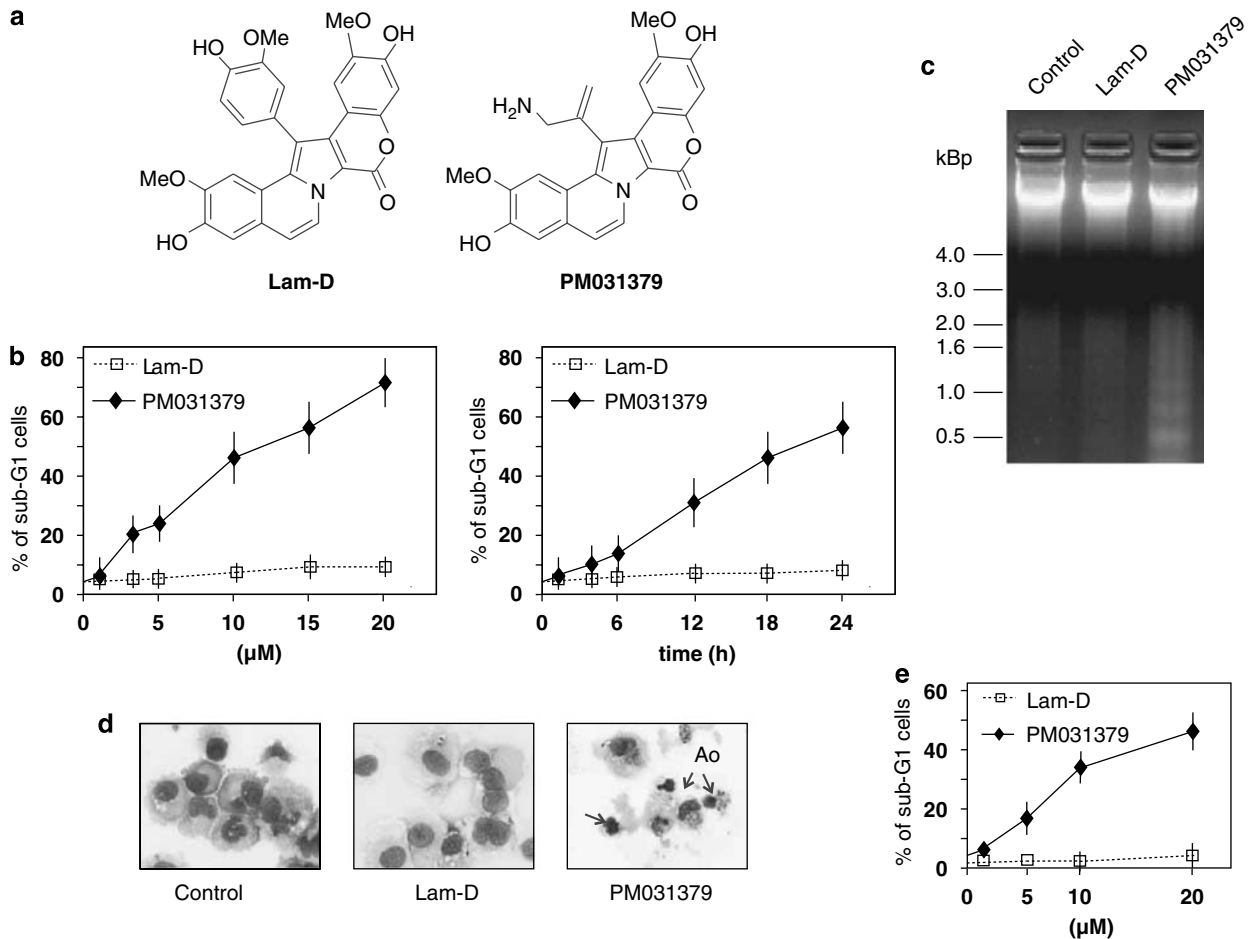


Figure 1 Nuclear signs of apoptosis induced by lamellarins. (a) Structure of Lam-D and PM031379. (b) For the concentration-dependent study (left), U1810 cells were treated with 1, 3, 5, 10, 15 and 20 μM of Lam-D or PM031379 for 18 h and the percentage of sub-G1 cells was measured by flow cytometry. Results are representative of four independent experiments. For the time-dependent study (right), U1810 cells were treated with 10 μM of Lam-D or 10 μM PM031379 for 1, 4, 6, 12, 18 and 24 h and the percentage of sub-G1 cells was determined as above. (c and d) U1810 cells were cultured for 18 h in the absence (Control) or presence of 10 μM Lam-D or 10 μM PM031379. (c) The internucleosomal DNA fragmentation was assessed by agarose gel electrophoresis followed by ethidium bromide staining. (d) Morphological studies were performed after May Grunwald Giemsa staining (original magnification × 630; arrows indicate cells with the morphological appearance of apoptosis). (e) Apoptosis induced by lamellarins in A549 cells. The human lung adenocarcinoma cells, A549, were cultured for 24 h with indicated concentrations of Lam-D or PM031379 and the percentage of sub-G1 cells was determined. Results are representative of three independent experiments. Lam-D, lamellarin-D.

(Figure 2b) as well as the activation of effector caspases (Figure 2c). It is noteworthy that although Lam-D failed to induce nuclear apoptosis of U1810 cells, Lam-D and PM031379 demonstrated equipotent effects on activation of the first steps of the apoptotic cascade. Thus, we considered the possibility that the apoptosis-inducing cascade stimulated by Lam-D would be interrupted downstream the mitochondrial outer membrane permeabilization and caspase activation steps but upstream of the nuclear apoptotic events. Hence, we examined the subcellular distribution of AIF upon Lam-D and PM031379 exposure (Figure 2d). Consistent with the results of immunoblots (Figure 2b), confocal microscopic analysis showed the translocation of AIF from mitochondria to the cytosol in response to Lam-D or PM031379 administration as indicated by the diffuse extra nuclear staining pattern observed in comparison to control cells (Figure 2d). However, PM031379 differed in its capacity to trigger the nuclear translocation of

AIF. While PM031379 was efficient in stimulating the translocation of AIF to the nucleus, Lam-D failed to do so (Figure 2d). Thus, the capacity of PM031379 (as opposed to Lam-D) to induce nuclear pyknosis and karyorrhexis correlates with its unique potential to induce the complete mitochondrio-nuclear translocation of AIF (Figure 2d). It appears that translocation of AIF to the nucleus is a critical step for the development of the apoptotic process in lung cancer.

Involvement of AIF-mediated pathway in PM03137-induced U1810 cell apoptosis

To evaluate the contribution of AIF-dependent and caspases-dependent cell death pathways in PM031379-treated U1810 cells, AIF was silenced by siRNA or caspases were inhibited by addition of *N*-benzyloxycarbonyl-Val-Ala-Asp(Ome)-fluoromethylketone (*Z*-VAD-fmk). Then, apoptosis and clonogenic cell survival were

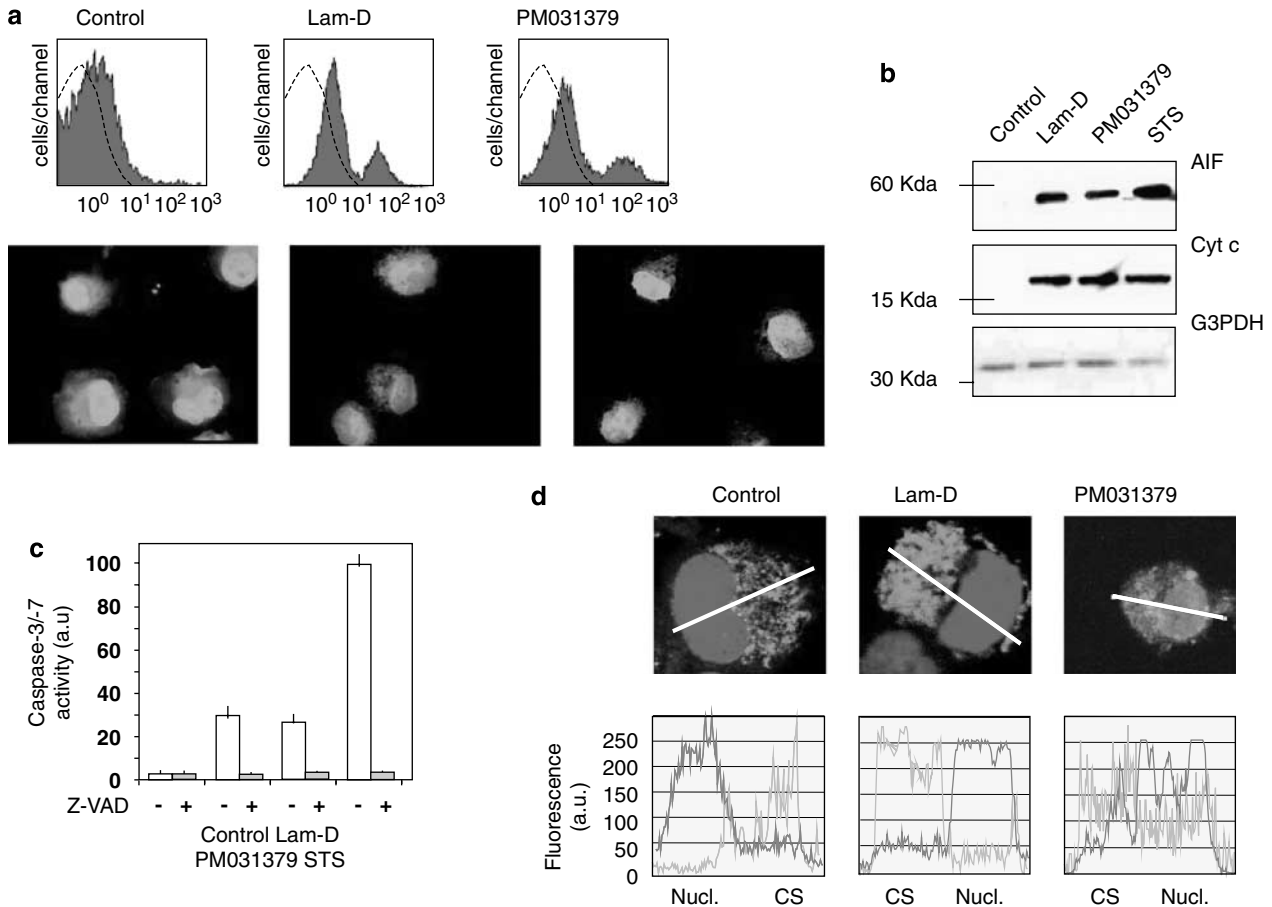


Figure 2 Apoptotic signaling pathways triggered by Lam-D and PM031379. (a) Bax activation and its mitochondrial membrane localization were assessed following treatment with 10 μ M PM031379 or Lam-D for 6 h. Upper panel, intracellular flow cytometry was performed using conformation-specific anti-Bax antibody (solid line) as described. Secondary antibody alone served as negative control (dashed line). Lower panel, microscopy examination of the subcellular localization of Bax using specific immunostaining (original magnification \times 630). (b) Mitochondrial release of Cyt *c* and AIF upon Lam-D and PM031379 exposure. Eighteen hours after the treatment with 10 μ M Lam-D, 10 μ M PM031379, or 1 μ M STS, the cytosolic fractions were analysed by immunoblot using specific antibodies. G3PDH served as loading control. Data are representative of three independent experiments. (c) Caspase-3/-7 activity in U1810 cells treated with lamellarins. Cells were incubated with 10 μ M PM031379, 10 μ M Lam-D or 1 μ M STS for 18 h in the presence or absence of the caspase inhibitor *N*-benzyloxycarbonyl-Val-Ala-Asp(Ome)-fluoromethylketone (Z-VAD, 100 μ M) (means \pm s.d. of three independent experiments performed in duplicate). (d) Confocal images of immunostaining with AIF (green) and nuclear PI staining (red) of U1810 cells treated or not treated (control) with 10 μ M Lam-D or 10 μ M PM031379 for 18 h (upper panel). Quantification of signals was also measured by confocal microscopy (lower panel). The fluorescence intensities of cells (AIF: green; PI: red) were measured along the cursor (white line, upper panel). Data are shown on a linear scale of arbitrary units of fluorescence intensity for different subcellular regions. Two additional studies yielded similar results. Lam-D, lamellarin-D; Cyt *c*, cytochrome *c*; AIF, apoptosis-inducing factor; STS, staurosporine; Z-VAD, *N*-benzyloxycarbonyl-Val-Ala-Asp(Ome); CS, cytoplasm; Nucl, nucleus.

assessed upon treatment with PM031379 (Figure 3). AIF siRNA, which reduced the expression of protein by 70% (Figure 3a), Z-VAD-fmk, both significantly decreased hypoploidy (sub-G1) induced by PM031379 as an internal control of their efficacy (Figure 3b). Confirming with the seminal role of AIF in lung cancer cell death (Gallego *et al.*, 2004), the death of U1810 cells induced by PM031379 was largely prevented when AIF was silenced (Figure 3b). Although Z-VAD-fmk completely inhibited caspase-3/-7 activity in U1810 cells treated with PM031379 (Figure 2c and not shown), it failed to counteract the lethal effect of PM031379 (Figure 3b). Thus, the induction of cell death by PM031379 in U1810 cells was largely mediated by the AIF-dependent pathway and caspases were required for

the nuclear DNA loss, yet were dispensable for the occurrence of cell death.

Since AIF has a physiological role for the maintenance of complex I of the respiratory chain (Vahsen *et al.*, 2004), the knockdown of AIF might result in PM031379 resistance due to adventitious effects on the AIF-dependent mitochondrial function and not to the pro-apoptotic function of AIF. To exclude this possibility, we used a second approach to interfere with the pro-apoptotic function of AIF. U1810 cells were microinjected with a neutralizing anti-AIF antibody that is able to prevent AIF translocation to the nucleus (Gallego *et al.*, 2004) or an isotype-matched anti-CD86 control antibody (Figure 3c). Upon treatment with PM031379, 49% of U1810 cells microinjected with control antibody

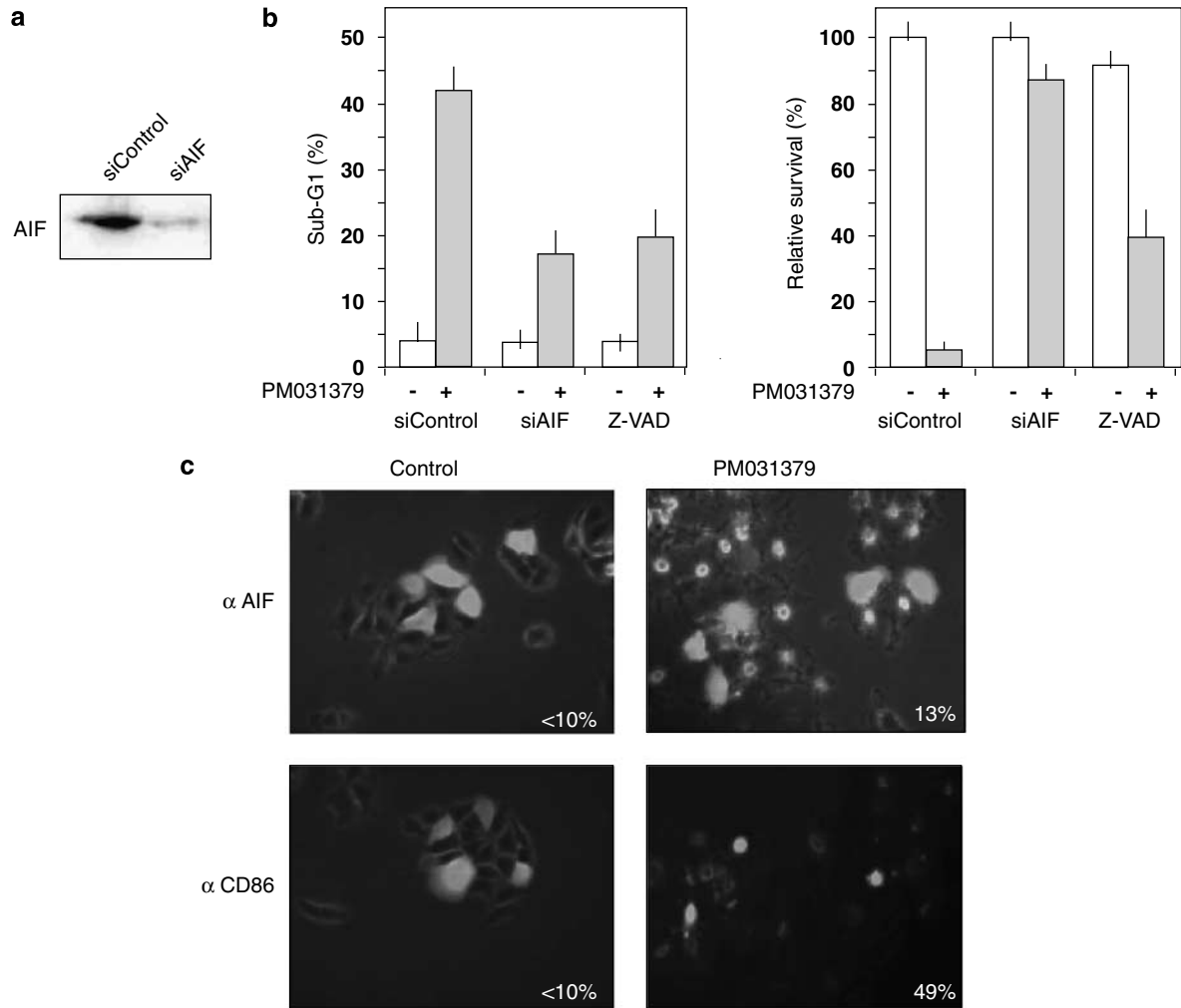


Figure 3 Effect of AIF depletion on hypoploidy and cell survival reduction induced by PM031379. **(a and b)** AIF was depleted in U1810 cells using siRNA. U1810 cells were electroporated with AIF siRNA (siAIF) or control siRNA (siControl). **(a)** Immunoblots of AIF expression in U1810 cells 72 h after electroporation with indicated siRNA. Equal loading was confirmed by probing with a G3PDH-specific antibody. **(b)** Fifty-four hours after transfection, cells were left untreated or treated with 10 μ M PM031379 in the presence or absence of 100 μ M Z-VAD-fmk for 18 h. Then, the frequency of cells with a subdiploid DNA content (left) or the relative survival (right) was determined. The percentage of sub-G1 was determined by flow cytometry (means \pm s.d. of three independent experiments). Survival was assessed by colony forming assays (means \pm s.d. of three independent experiments, each performed in duplicate). **(c)** Representative images of U1810 cells microinjected with either a neutralizing antibody against AIF or an isotype matching antibody (antibody against CD86) used as control along with dextran-Alexa and then treated or not treated with 10 μ M PM031379. Eighteen hours later, cells were observed under the microscope and the fraction of dextran-Alexa-positive cells (green fluorescence) exhibiting a death phenotype (arrows) was scored. Numbers represent the percentage of dead cells. siRNA, small interfering RNA; siAIF, small interfering apoptosis-inducing factor; Z-VAD-fmk, *N*-benzyloxycarbonyl-Val-Ala-Asp(Ome)-fluoromethylketone.

presented morphological signs of cell death. In contrast, anti-AIF microinjection largely prevented the PM031379-induced cytotoxicity, down to 13%, 18 h after PM031379 treatment. This experiment confirms that AIF translocation to the nucleus is necessary for PM031379-mediated apoptosis of U1810 cells.

Mitochondrial ROS production is crucial for PM031379-induced U1810 cell apoptosis

Because the oxidative balance is thought to influence the resistance to apoptosis induced by anticancer drugs in lung cancer (Kang *et al.*, 2004a), we subsequently measured the production of intracellular ROS in

U1810 cells, before and after treatment with Lam-D or PM031379. This was performed by using the superoxide-sensitive probe hydroethidine (HE), a non-fluorescent chemical that enters cells and that can be oxidized to fluorescent hydrophilic ethidium, which then is trapped within the cellular membranes. As shown in Figure 4a, ROS levels were increased after treatment with PM031379, and this increase was efficiently blocked by pretreatment with the thiol containing antioxidant *N*-acetyl cystein (NAC). Similar inhibitory effects were observed with the antioxidant compounds, α -tocopherol and L-ascorbate but with a reduced efficacy (Figure 4a). The increase in ROS level became obvious within 2 h after PM031379 exposure (Figure 4b),

well before signs of apoptosis occur (Figure 1b). Using the peroxide-specific probe dichlorofluorescein diacetate, similar increases in ROS level were observed upon PM031379 exposure (not shown). In contrast to PM031379, however, Lam-D was unable to trigger the generation of ROS (Figure 4a). To determine whether mitochondria were the source of ROS induced by PM031379, we measured the HE-detectable ROS in normal U1810 cells as well as cells that were depleted from mitochondrial DNA and that bear a so-called ρ^0 phenotype (Figure 4B). ρ^0 cells lack mitochondrial DNA-encoded proteins and RNAs and are incapable of mitochondrial respiration (not shown) because of the loss of key components of the electron transport chain. In contrast to normal U1810 cells, ρ^0 U1810 cells failed to exhibit a consistent increase in HE fluorescence over 24 h of PM031379 exposure contrasting with graded increases in ROS generation observed in U1810 cells (Figure 4b). Thus, an intact respiratory chain is essential for the ROS generation induced by PM031379 in NSCLC cells.

Since glutathione (GSH) is a major antioxidant that plays a key role in maintaining the intracellular redox state (Anderson *et al.*, 1997), we therefore determined a kinetic analysis of the effects of PM031379 on intracellular levels of GSH (Figure 4c). Treatment with PM031379 resulted in a slight increase in cellular GSH detected 3 h after PM031379 exposure then the GSH levels remained almost unchanged. Cells were incubated with the thiol-reacting agent, *N*-ethylmaleimide or with L-buthionine sulfoximine, a specific inhibitor of GSH synthesis, providing a control for GSH depletion (Figure 4c). These observations led us to conclude that elevation of ROS induced by PM031379 was not due to a decrease in antioxidant capacity.

Next, we investigated the extent to which mitochondrial ROS production contributed to apoptosis of U1810 cells. Inhibition of ROS by NAC prevented nuclear apoptosis induced by PM031379 (Figure 4d). In agreement, the antioxidants, α -tocopherol and L-ascorbate reduced the percentage of apoptotic cells upon PM031379 exposure (Figure 4d). Moreover, ρ^0 U1810 cells, which have lost their ability to produce mitochondrial ROS in response to PM031379 administration (Figure 4b), were resistant against PM031379-induced

apoptosis (Figure 4c). These observations support the notion that mitochondrial ROS are required for efficient apoptosis of NSCLC cells.

Mitochondrial ROS are involved in AIF nuclear translocation

Since it has been reported that the mitochondrial AIF redistribution is modulated by intracellular ROS level (Murahashi *et al.*, 2003; Park *et al.*, 2005a), we investigated to which extent ROS affect the subcellular redistribution of AIF from mitochondria to the cytosol and then to the nucleus. The antioxidant NAC that suppressed nuclear apoptosis (Figure 3c) failed to prevent the mitochondrial release of the pro-apoptotic proteins Cyt *c* or AIF as well as the activation of caspase-3 (Figure 5a). However, in conditions in which NAC inhibited ROS production (Figure 4a) and cell death (Figure 4c), NAC also largely prevented the PM031379-induced AIF nuclear translocation (Figure 5a) and the fragmentation of nuclear DNA in high molecular weight fragments (Figure 5b) that is a typical hallmark of AIF activity in the nucleus (Susin *et al.*, 2000). Similarly, nuclear translocation of AIF was absent in ρ^0 U1810 cells exposed to PM031379 (Figure 5c). Moreover, pre-incubation of U1810 cells with menadione, a substance known to generate ROS by futile redox cycles in mitochondria, restored the capacity of Lam-D to induce nuclear translocation of AIF (Figure 6a). These results suggest that mitochondrial ROS induced by PM031379 are required for the nuclear translocation of AIF providing a mechanistic explanation for the involvement of mitochondrial ROS in U1810 cells apoptosis.

Menadione enhances the susceptibility of U1810 cells to apoptosis induction

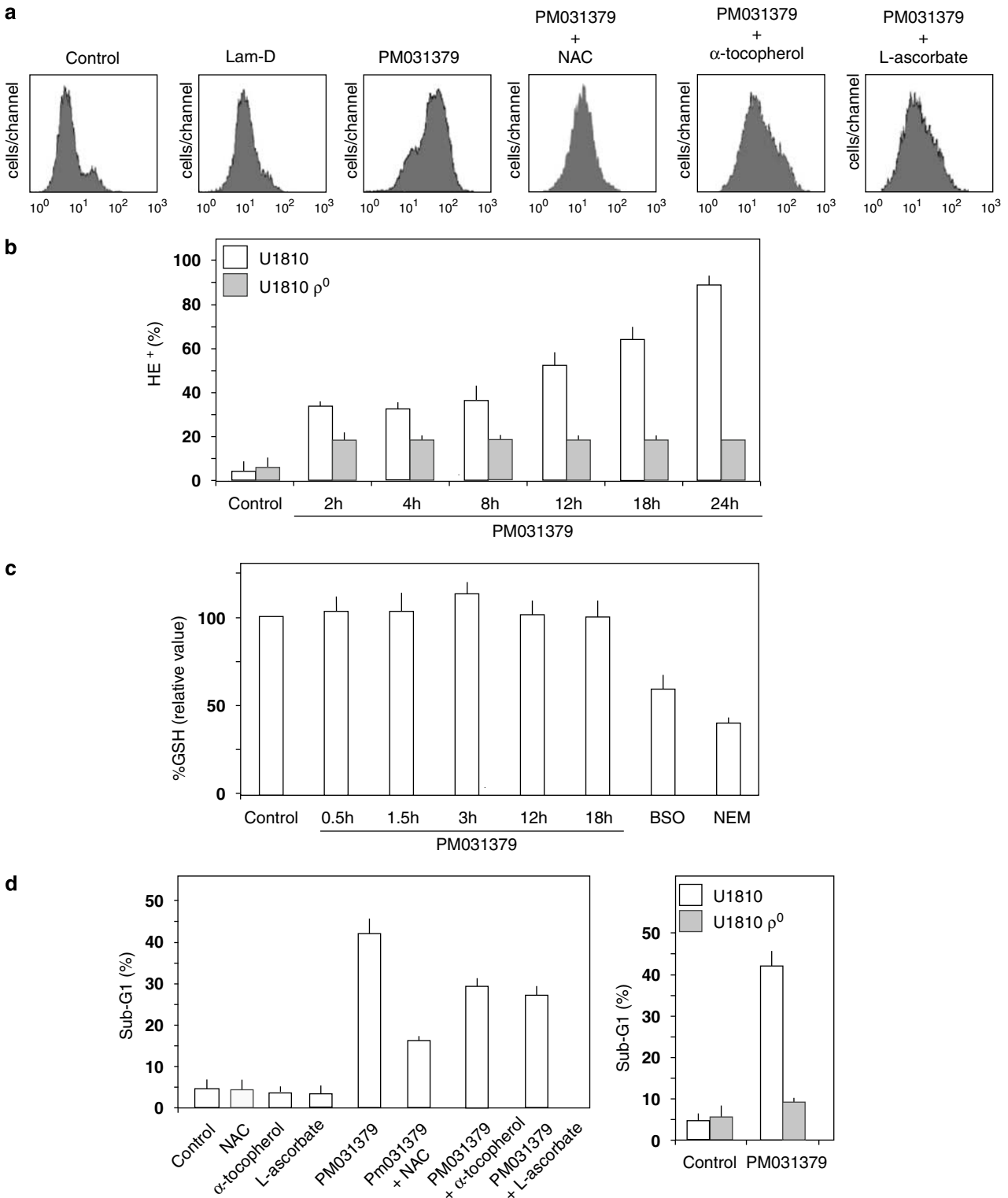
We next examined the effect of intracellular ROS production in combination with Lam-D or DNA damaging agents on NSCLC cell death. Confirming previous data (Joseph *et al.*, 2001; Ekedahl *et al.*, 2003), U1810 cells are resistant to apoptosis induction by the conventional chemotherapeutic drugs etoposide and cisplatin as well as Lam-D (Figure 6b). Incubation of U1810 cells with menadione resulted in moderate

Figure 4 ROS production in Lam-D and PM031379-treated U1810 cells. (a) U1810 cells were pretreated in the absence or presence of 10 mM NAC for 30 min, 100 μ M L-ascorbate or 100 μ M α -tocopherol for 2 h. Then cells were incubated with dimethylsulfoxide (Control), 10 μ M Lam-D or 10 μ M PM031379 for 18 h. Finally, cells were labeled with hydroethidine and subjected to cytofluorometric analysis. The experiment was conducted twice with similar results. (b) Kinetics of the PM031379-induced ROS production in U1810 cells and U1810 ρ^0 cells. U1810 ρ^0 cells and the parental wild-type U1810 cells were incubated in the presence of 10 μ M PM031379 for the indicated period, and the percentage of HE⁺ cells (mean \pm s.d. of three independent experiments) was determined by flow cytometry. (c) Intracellular GSH level in U1810 cells after PM031379 exposure. U1810 cells were incubated in the presence of 10 μ M PM031379 for the indicated period, and the levels of glutathione were determined. Alternatively, U1810 cells were treated with 10 mM BSO or with 100 μ M NEM for 12 h to deplete intracellular GSH. Results are expressed as fluorescence as a percentage of control (mean \pm s.d. of three independent experiments in triplicates). (d) Effect of inhibition of ROS production on PM031379-induced apoptosis. U1810 cells were pretreated or not pretreated with NAC (10 mM) for 30 min, L-ascorbate (100 μ M) or α -tocopherol (100 μ M) for 2 h and then cells were incubated with dimethylsulfoxide (Control) or 10 μ M PM031379 for 18 h (left part). Nuclear apoptosis was determined by cytofluorometric analysis of the percentage of sub-G1 cells. Alternatively, the percentage of sub-G1 cells was determined in U1810 ρ^0 cells and in the parental wild-type U1810 cells treated with 10 μ M PM031379 for 18 h (right part). ROS, reactive oxygen species; Lam-D, lamellarin-D; NAC, *N*-acetyl cysteine; NEM, *N*-ethylmaleimide; BSO, *N*-buthionine sulfoximine; GSH, glutathione.

apoptosis (Figure 6b). However, pretreatment with menadione increased the susceptibility of the cells to the lethal effects of Lam-D as well as etoposide or cisplatin (Figure 6b). Taken together, these data suggest that the drug-induced generation of mitochondrial ROS may sensitize NSCLC cells to apoptosis induction.

Discussion

Platinum-based chemotherapies are widely used as a first-line treatment of NSCLC. However, low response rates to platinum-based chemotherapies illustrate that resistance to current therapies is a crucial problem in



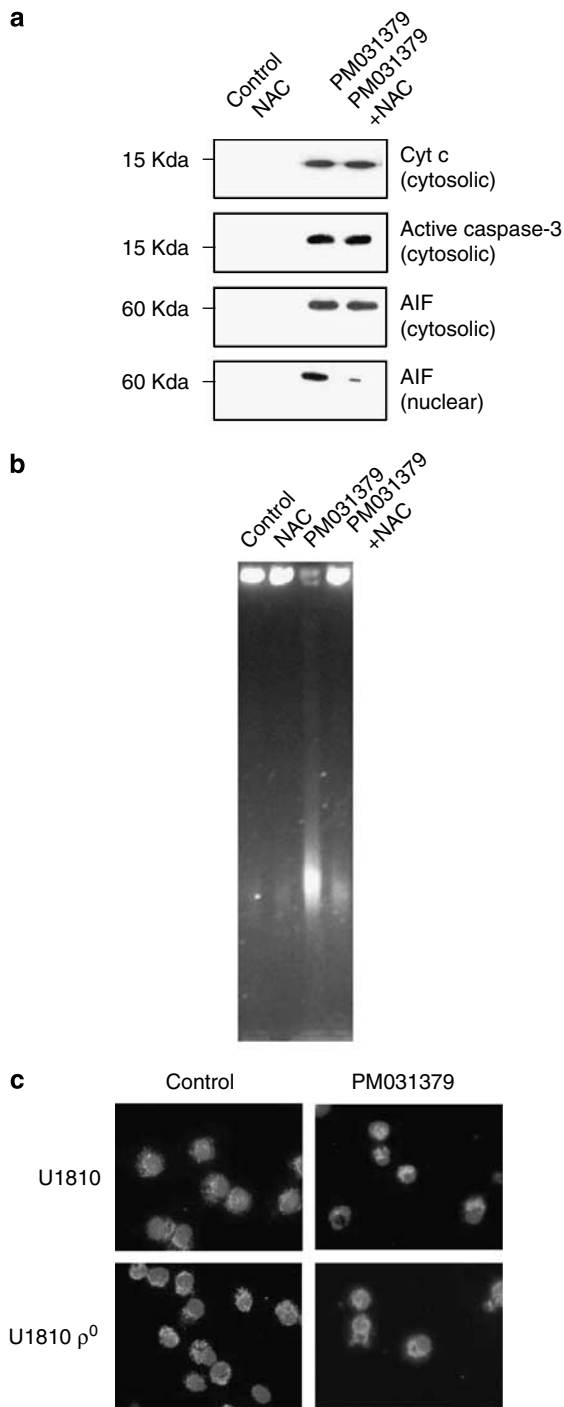


Figure 5 Effect of ROS inhibition on the subcellular redistribution of pro-apoptotic proteins. **(a)** Cytosolic and nuclear fractions were obtained from U1810 cells treated with 10 μ M PM031379 for 18 h. Where indicated, cells were pre-incubated for 2 h with NAC (10 mM) before PM031379 treatment. Subcellular fractions were subjected to immunoblot detection of Cyt *c*, active caspase-3 and anti-AIF. **(b)** Genomic DNA analysed by pulse field gel electrophoresis. The effect of NAC (10 mM) on large-scale DNA fragmentation in PM031379 (10 μ M)-treated U1810 cells were analysed at 24 h. **(c)** Representative images of immunostaining of AIF (green) and nuclear Hoechst 33342 (blue) staining of U1810 ρ^0 cells and the parental wild-type U1810 cells treated with 10 μ M PM031379 for 18 h (original magnification \times 630). ROS, reactive oxygen species; NAC, *N*-acetyl cysteine; Cyt *c*, cytochrome *c*; AIF, apoptosis-inducing factor.

NSCLC management. Cytotoxic agents often trigger the caspase-mediated mitochondrial cell death pathway. However, multiple results suggest that the classical caspase-dependent apoptotic pathways are not functional in NSCLC cells in response to cytotoxic agents *in vitro* (Yang *et al.*, 2003; Bartling *et al.*, 2004; Broker *et al.*, 2004) and this may also be the case *in vivo* (Ferreira *et al.*, 2001a, b). As an example, chemoresistant NSCLC exhibit a reduced expression of caspase-9 or caspase-3 (Okouoyo *et al.*, 2004). We previously identified the U1810 cells as the most radioresistant among a panel of NSCLC cell lines (Joseph *et al.*, 2001). However, the resistance of U1810 cells cannot simply be explained by the absence of apoptotic proteins or the overexpression of anti-apoptotic proteins (Joseph *et al.*, 2001).

One therapeutic option that has been proposed to overcome resistance is the restoration of the defective caspase-dependent cell death pathway (Fennell, 2005). Overexpression of caspases in drug-resistant human NSCLC xenografts may overcome chemoresistance *in vivo* (Okouoyo *et al.*, 2004). Pharmacological inhibition of IAP proteins restored NSCLC cells apoptosis sensitivity *in vitro* and *in vivo*, in mice grafted with human NSCLC (Yang *et al.*, 2003). Other therapeutic strategy consists in stimulating caspase-independent cell death pathways in NSCLC. Indeed, cell death can occur in caspase-deficient cells through the activation of caspase-independent routes. Thus, microtubule-stabilizing agents trigger cell death through pathway involving the lysosomal protease cathepsin B in NSCLC resistant to DNA-damaging agents (Broker *et al.*, 2004). Alternatively, nuclear translocation of AIF may be crucial in determining the chemosensitivity of NSCLC cells (Gallego *et al.*, 2004, and this study). The nuclear translocation of AIF is an essential step for cell death induction since the presence of AIF in the nucleus (but not in the cytosol) is the parameter that predicts whether nuclear chromatin condensation as well as cell death occurs. This nuclear translocation is the only phenomenon that distinguishes the cellular effects of Lam-D and PM031379. While PM031379 induces nuclear AIF translocation, apoptosis and cell death, Lam-D fails to do so. Moreover, the PM031379-induced cell death is prevented by several antioxidants or depletion of mitochondrial DNA at the level of the nuclear translocation of AIF. As we demonstrated in this study, the generation of ROS induced by PM031379 was not accompanied by depletion of GSH content. Moreover GSH depletion by L-buthionine sulfoximine did not induce U1810 cell death (not shown). Thus, such an ROS accumulation and cell death are apparently unrelated to the rate of glutathione.

The present study suggests a novel strategy to restore apoptosis in chemoresistant NSCLC cells. We demonstrated that mitochondrial ROS favors the apoptosis by stimulating the nuclear translocation of AIF. Consistent with these findings, ROS generation has been involved in lung cancer cell death via a caspase-independent pathway (Kang *et al.*, 2004a). We used lamellarins as selective pharmacological tools to activate mitochondrial

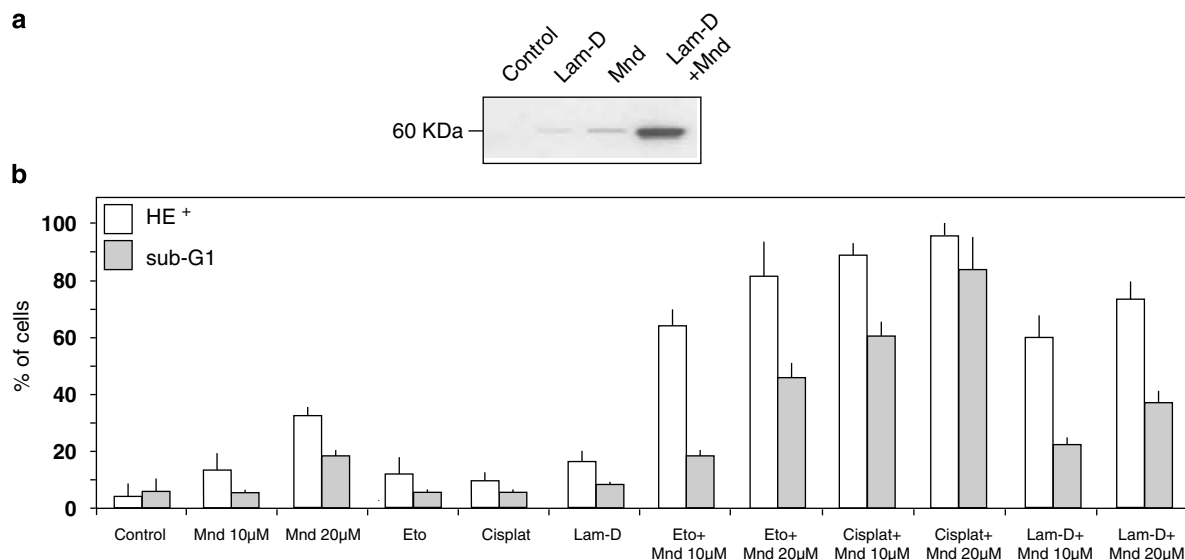


Figure 6 Effect of menadione in combination with the anticancer drugs Lam-D, etoposide and cisplatin on ROS production and apoptosis. (a) Nuclear redistribution of AIF was studied by immunoblot. Nuclear extracts were prepared from U1810 cells treated with 10 µM Lam-D alone or in combination with 20 µM Mnd for 18 h. Representative picture from two independent experiments. (b) U1810 cells were treated with 10 or 20 µM Mnd alone or in combination with 10 µM Lam-D or 10 µM Eto or 40 µM Cisplat for 18 h. Cells were harvested for determination of apoptosis (% of sub-G1 cells) and ROS generation (HE⁺) (means ± s.d. of three independent experiments). Lam-D, lamellarin-D; ROS, reactive oxygen species; AIF, apoptosis-inducing factor; Mnd, menadione; Eto, etoposide; Cisplat, cisplatin; HE, hydroethidine.

cell death pathways. Indeed, we have found that Lam-D and PM031379 are potent mitochondria-targeted agents triggering mitochondrial permeability transition and subsequent apoptosis in a large panel of tumor cells (Kluza *et al.*, 2006). Mitochondrial respiration is associated with the generation of small amounts of ROS, and it is generally taken as an established fact that mitochondrial permeability transition responsible for uncoupling of mitochondrial electron transport causes increased generation of ROS (Zamzami *et al.*, 1995). Surprisingly, we did not observe any mitochondrial ROS production with the mitochondrial permeability transition inducer Lam-D (Figure 3). This may be due to intrinsic antioxidant properties of Lam-D as already seen with other lamellarin alkaloids (Krishnaiah *et al.*, 2004). However, we were unsuccessful to demonstrate the antioxidant capability of Lam-D in U1810 cells (data not shown). From a pharmacological point of view, lamellarins represent a promising family of anticancer agents due to their potent activities in xenograft models and their original mechanism of action and the present work strongly reinforces the idea that Lam-D and PM031379 exhibit distinct mechanistic properties (Bailly, 2004). Lam-D derivatives are now designed as topoisomerase I-targeted agents, whereas amino analogs of the PM031379-type essentially function as ROS-promoting mitochondriotoxic agents. These molecules are excellent tools to dissect the apoptotic machinery and solid anticancer drug candidates. The pre-clinical development of a lamellarin derivative is currently ongoing.

To conclude, the importance of promoting mitochondrial ROS could determine the chemosensitivity of

NSCLC cells. The enhancement of drug sensitivity with increased intracellular ROS level may provide an opportunity to develop novel strategies to fight against cancer.

Materials and methods

Chemicals and modulation of apoptosis

Staurosporine, *N*-ethylmaleimide, L-buthionine sulfoximine, NAC, α -tocopherol (vitamin E) and 100 µM L-ascorbate (vitamin C) were purchased from Sigma (St Louis, MO, USA). Lam-D and PM031379 were synthesized at Pharmamar (Madrid, Spain). Compounds were dissolved in dimethylsulfoxide at an initial stock concentration of 10 mM and stored at -20°C in the dark. Subsequent dilutions were performed in phosphate-buffered saline or in culture medium. When indicated, cells were treated with cisplatin or etoposide (both from Bristol-Myers Squibb, New York, NY, USA) alone or in combination with menadione (Sigma). Z-VAD-fmk (Bachem, Basel, Switzerland) was used at 100 µM.

Culture conditions and generation of siRNA

The characterized human NSCLC cell line U1810 (Bergh *et al.*, 1985) was routinely cultivated as published (Gallego *et al.*, 2004). We applied siRNA to inhibit AIF expression using an siRNA double-stranded oligonucleotide designed to interfere with the expression of human AIF (sense anti-human AIF 5'-GAUCCUCCCCGAAUACCUCTT-3', Proligo, Boulder, CO, USA). An oligonucleotide-specific for mouse AIF (sense anti-mouse AIF 5'-AUGCAGAACUCCAAGCACGTT-3') that does not affect human AIF was used as a control as reported before (Cande *et al.*, 2004). Exponentially growing cells were concentrated to 10⁷ cells ml⁻¹ in optiMEM medium (Invitrogen, Cergy-Pontoise, France) and 500 µl of cell

suspension was pipetted into a 4-mm electroporation cuvette (Cell Projects, Marietsham, UK), then siRNAs were added at a final concentration of 150 pmol. Electroporation was performed immediately with an Easyject Electroporator (Equibio, Flowgen, Nottingham, UK) using a rectangle pulse of 260 V, 900 μ F. After incubating for 15 min at RT, the cells were diluted with culture medium and incubated for 72 h before experiments. Silencing of AIF was determined by measuring AIF protein expression at 72 h after electroporation by immunoblotting.

Generation of ρ^0 cells

The procedure to generate ρ^0 cells was based on standard published protocols using ethidium bromide (Marchetti *et al.*, 1996b). Two different sublines were derived and controlled for mtDNA depletion using specific PCR reactions as described elsewhere (Armand *et al.*, 2004). The ρ^0 subline that morphologically resembled most closely the parental wild-type control cell line was kept and results are shown for this cell line. In experiments, ρ^0 and parental wild type control cells were maintained in the same culture medium supplemented with pyruvate, uridine and glucose. Twenty-four hours before experiments were realized, ethidium bromide was removed from the medium of ρ^0 cells.

Detection of apoptosis

The frequency of hypoploid cells (sub-G1 cells) was assessed as described (Gallego *et al.*, 2004). DNA fragmentation (5×10^6 cells per lane) was determined by agarose gel electrophoresis as described previously (Kawabe and Ochi, 1991). Formation of high molecular weight DNA fragments was determined by using pulse field gel electrophoresis, as described previously (Gallego *et al.*, 2004). The activity of caspase-3-like enzymes was determined with the Caspase-Glo 3/7 luminescent kit (Promega Corp, Madison, WI, USA) according to the manufacturer's recommendation.

Cytofluorometric analysis of ROS production

To evaluate the intracellular production of ROS, cells were incubated for 15 min at 37°C to 500 nm HE immediately before cytofluorometric analysis as previously described (Marchetti *et al.*, 1996a).

Determination of intracellular glutathione

The total glutathione content was determined after loading the cells with the glutathione sensitive probe, monochlorobimane. U1810 cells were seeded at a density of 5×10^4 per well into 96-well black microtiter plates in triplicates. After 8 h of incubation at 37°C in 5% CO₂, cells were treated for various period of time. Then, monochlorobimane (100 μ l) in phosphate-buffered saline was added at a final concentration of 40 μ M to the living cells and left 30 min. Fluorescence was measured at 460 nm using a microplate-reading fluorometer (Fluorocount, Packard Instrument Company, Meriden, CT, USA) with excitation at 360 nm.

Clonogenic assay

U1810 cells were seeded into 25-cm² flasks and allowed to grow until sub-confluence. U1810 cells were treated for 18 h with Z-VAD-fmk (100 μ M), PM031379 (10 μ M) alone or in combination with Z-VAD-fmk. Alternatively, 54 h after electroporation, siControl or siAIF U1810 cells were treated next with 10 μ M PM031379 for 18 h. At the end of the incubation time, cells were collected from the monolayer with trypsin and washed twice in RPMI medium. The cells ($50\,000\text{ ml}^{-1}$) were plated in drug-free medium in triplicate into six-well dishes.

One week after treatment, the colonies that emerged in the Petri dish were stained with 0.2% crystal violet in 900 ml methanol to allow macroscopic estimation. The surviving fractions following given treatments were calculated as a percentage of viable cells in untreated cultures.

Immunofluorescence and Bax detection

For subcellular localization of AIF, U1810 cells were grown on coverslips and stained with AIF antibodies as described previously (Gallego *et al.*, 2004). For counterstaining, propidium iodide (0.2 $\mu\text{g ml}^{-1}$) or Hoechst 33342 (10 $\mu\text{g ml}^{-1}$) was used. All samples were analysed using a confocal microscope (Leica TCS NT, Leica Microsystems, Rueil-Malmaison, France) as described (Gallego *et al.*, 2004).

For flow cytometric analysis of Bax activation, a procedure described elsewhere (Nyman *et al.*, 2005) was used. Then cells (10 000 per sample) were analysed on a XL flow cytometer. Alternatively, the subcellular localization of Bax was detected by immunofluorescence using anti-human Bax antibody (dilution 1:200, clone 2D2; AG Scientific, San Diego, CA, USA). Primary antibody binding was detected with Alexa Fluor 488-conjugated anti-mouse antibodies (dilution 1:500). Samples were viewed using fluorescence microscope DMLR (Leica).

Immunoblot analysis

Cytosolic fractions or cytosols were prepared using a method that has been reported previously (Gallego *et al.*, 2004). Nuclear extracts were prepared using the Nuclear Fractionation kit (Biovision, Mountain View, CA, USA). Fifty micrograms of proteins of the cytosolic fraction or the nuclear extract were subjected to 12% SDS-PAGE and transferred onto nitrocellulose membranes (Amersham Life Science, Buckinghamshire, UK) which were afterwards probed with primary antibodies including anti-Cyt *c*, clone 7H8.2C12 (1/1000; BD Biosciences Pharmingen, San Diego, CA, USA), anti-AIF (1:1000, sc-13116; Santa Cruz Biotechnology Inc., Santa Cruz, CA, USA) and anti-active caspase-3 (1:1000; Cell Signalling, Danvers, MA, USA). Fractionation quality and protein loading were verified by the distribution of the specific subcellular markers: G3PDH using a rabbit anti-G3PDH (1:1000; Trevigen, Gaithersburg, MD, USA) for cytoplasm and Lamin B using a goat anti-Lamin B (1:5000; Santa Cruz) for nucleus. Primary antibodies binding was detected with horseradish peroxidase-conjugated-specific antibodies (1:1000; Biorad) and visualized by enhanced chemiluminescence following the manufacturer's instructions (Amersham Pharmacia Biotech, Piscataway, NJ, USA).

Abbreviations

AIF, apoptosis-inducing factor; Cyt *c*, cytochrome *c*; HE, hydroethidine; Lam-D, lamellarin-D; NAC, *N*-acetyl cystein; NSCLC, non-small cell lung carcinoma; ROS, reactive oxygen species.

Acknowledgements

We thank Pierre Cappy for technical help. In memoriam we like to acknowledge the contribution to this article from Martial Flactif who passed away in July 2006.

This work was supported by grants from INSERM, Université de Lille II, Ligue Nationale contre le Cancer Comité du nord (to PM), Ligue Nationale contre le Cancer (Equipe labellisée) and Institut National contre le Cancer, and European Union ChemoRes (to GK).

References

- Anderson CP, Tsai J, Chan W, Park CK, Tian L, Lui RM *et al.* (1997). Buthionine sulphoximine alone and in combination with melphalan (L-PAM) is highly cytotoxic for human neuroblastoma cell lines. *Eur J Cancer* **33**: 2016–2019.
- Armand R, Channon JY, Kintner J, White KA, Miselis KA, Perez RP *et al.* (2004). The effects of ethidium bromide induced loss of mitochondrial DNA on mitochondrial phenotype and ultrastructure in a human leukemia T-cell line (MOLT-4 cells). *Toxicol Appl Pharmacol* **196**: 68–79.
- Bailly C. (2004). Lamellarins, from A to Z: a family of anticancer marine pyrrole alkaloids. *Curr Med Chem Anticancer Agents* **4**: 363–378.
- Bartling B, Lewensohn R, Zhivotovsky B. (2004). Endogenously released Smac is insufficient to mediate cell death of human lung carcinoma in response to etoposide. *Exp Cell Res* **298**: 83–95.
- Bergh J, Nilsson K, Ekman R, Giovanella B. (1985). Establishment and characterization of cell lines from human small cell and large cell carcinomas of the lung. *Acta Pathol Microbiol Immunol Scand [A]* **93**: 133–147.
- Broker LE, Huisman C, Span SW, Rodriguez JA, Kruyt FA, Giaccone G. (2004). Cathepsin B mediates caspase-independent cell death induced by microtubule stabilizing agents in non-small cell lung cancer cells. *Cancer Res* **64**: 27–30.
- Cande C, Vahsen N, Metivier D, Tourriere H, Chebli K, Garrido C *et al.* (2004). Regulation of cytoplasmic stress granules by apoptosis-inducing factor. *J Cell Sci* **117**: 4461–4468.
- Ekedahl J, Joseph B, Marchetti P, Fauvel H, Formstecher P, Lewensohn R *et al.* (2003). Heat shock protein 72 does not modulate ionizing radiation-induced apoptosis in U1810 non-small cell lung carcinoma cells. *Cancer Biol Ther* **2**: 663–669.
- Engel RH, Evens AM. (2006). Oxidative stress and apoptosis: a new treatment paradigm in cancer. *Front Biosci* **11**: 300–312.
- Facompre M, Tardy C, Bal-Mahieu C, Colson P, Perez C, Manzanares I *et al.* (2003). Lamellarin D: a novel potent inhibitor of topoisomerase I. *Cancer Res* **63**: 7392–7399.
- Fennell DA. (2005). Caspase regulation in non-small cell lung cancer and its potential for therapeutic exploitation. *Clin Cancer Res* **11**: 2097–2105.
- Ferreira CG, van d V, Span SW, Jonker JM, Postmus PE, Kruyt FA *et al.* (2001a). Assessment of IAP (inhibitor of apoptosis) proteins as predictors of response to chemotherapy in advanced non-small-cell lung cancer patients. *Ann Oncol* **12**: 799–805.
- Ferreira CG, van d V, Span SW, Ludwig I, Smit EF, Kruyt FA *et al.* (2001b). Expression of X-linked inhibitor of apoptosis as a novel prognostic marker in radically resected non-small cell lung cancer patients. *Clin Cancer Res* **7**: 2468–2474.
- Furre IE, Shahzidi S, Luksiene Z, Moller MTN, Borgen E, Morgan J *et al.* (2005). Targeting PBR by hexaminolevulinium-mediated photodynamic therapy induces apoptosis through translocation of apoptosis-inducing factor in human leukemia cells. *Cancer Res* **65**: 11051–11060.
- Gabellini N, Masola V, Quartesan S, Oselladore B, Nobile C, Michelucci R *et al.* (2006). Increased expression of LGI1 gene triggers growth inhibition and apoptosis of neuroblastoma cells. *J Cell Physiol* **207**: 711–721.
- Gallego MA, Joseph B, Hemstrom TH, Tamiji S, Mortier L, Kroemer G *et al.* (2004). Apoptosis-inducing factor determines the chemoresistance of non-small-cell lung carcinomas. *Oncogene* **23**: 6282–6291.
- Galluzzi L, Larochette N, Zamzami N, Kroemer G. (2006). Mitochondria as therapeutic targets for cancer chemotherapy. *Oncogene* **25**: 4812–4830.
- Johnstone RW, Ruefli AA, Lowe SW. (2002). Apoptosis: a link between cancer genetics and chemotherapy. *Cell* **108**: 153–164.
- Joseph B, Ekedahl J, Lewensohn R, Marchetti P, Formstecher P, Zhivotovsky B. (2001). Defective caspase-3 relocalization in non-small cell lung carcinoma. *Oncogene* **20**: 2877–2888.
- Kang YH, Lee E, Choi MK, Ku JL, Kim SH, Park YG *et al.* (2004a). Role of reactive oxygen species in the induction of apoptosis by alpha-tocopherol succinate. *Int J Cancer* **112**: 385–392.
- Kang YH, Yi MJ, Kim MJ, Park MT, Bae S, Kang CM *et al.* (2004b). Caspase-independent cell death by arsenic trioxide in human cervical cancer cells: reactive oxygen species-mediated poly(ADP-ribose) polymerase-1 activation signals apoptosis-inducing factor release from mitochondria. *Cancer Res* **64**: 8960–8967.
- Kawabe Y, Ochi A. (1991). Programmed cell death and extrathymic reduction of Vb8+ CD4+ T cells in mice tolerant to *Staphylococcus aureus* anterotoxin B. *Nature* **349**: 245–248.
- Kluza J, Gallego MA, Loyens A, Beauvillain JC, Sousa-Faro JM, Cuevas C *et al.* (2006). Cancer cell mitochondria are direct proapoptotic targets for the marine antitumor drug lamellarin D. *Cancer Res* **66**: 3177–3187.
- Krishnaiah P, Reddy VLN, Venkataramana G, Ravinder K, Srinivasulu M, Raju TV *et al.* (2004). New lamellarin alkaloids from the Indian ascidian *Didemnum obscurum* and their antioxidant properties. *J Nat Prod* **67**: 1168–1171.
- Marchetti P, Susin SA, Decaudin D, Gamen S, Castedo M, Hirsch T *et al.* (1996a). Apoptosis-associated derangement of mitochondrial function in cells lacking mitochondrial DNA. *Cancer Res* **56**: 2033–2038.
- Marchetti P, Zamzami N, Susin SA, Petit PX, Kroemer G. (1996b). Apoptosis of cells lacking mitochondrial DNA. *Apoptosis* **1**: 119–125.
- Murahashi H, Azuma H, Zamzami N, Furuya KJ, Ikebuchi K, Yamaguchi M *et al.* (2003). Possible contribution of apoptosis-inducing factor (AIF) and reactive oxygen species (ROS) to UVB-induced caspase-independent cell death in the T cell line Jurkat. *J Leukoc Biol* **73**: 399–406.
- Nyman U, Sobczak-Pluta A, Vlachos P, Perlmann T, Zhivotovsky B, Joseph B. (2005). Full-length p73{alpha} represses drug-induced apoptosis in small cell lung carcinoma cells. *J Biol Chem* **280**: 34159–34169.
- O'Connor K, Gill C, Tacke M, Rehmann FJ, Strohhfeldt K, Sweeney N *et al.* (2006). Novel titanocene anti-cancer drugs and their effect on apoptosis and the apoptotic pathway in prostate cancer cells. *Apoptosis* **11**: 1205–1214.
- Okouoyo S, Herzer K, Ucur E, Mattern J, Krammer PH, Debatin KM *et al.* (2004). Rescue of death receptor and mitochondrial apoptosis signaling in resistant human NSCLC *in vivo*. *Int J Cancer* **108**: 580–587.
- Park MT, Kim MJ, Kang YH, Choi SY, Lee JH, Choi JA *et al.* (2005a). Phytosphingosine in combination with ionizing radiation enhances apoptotic cell death in radiation-resistant cancer cells through ROS-dependent and -independent AIF release. *Blood* **105**: 1724–1733.
- Park YC, Jeong JH, Park KJ, Choi HJ, Park YM, Jeong BK *et al.* (2005b). Sulindac activates nuclear translocation of AIF, DFF40 and endonuclease G but not induces oligonucleosomal DNA fragmentation in HT-29 cells. *Life Sci* **77**: 2059–2070.

- Susin SA, Daugas E, Ravagnan L, Samejima K, Zamzami N, Loeffler M *et al.* (2000). Two distinct pathways leading to nuclear apoptosis. *J Exp Med* **192**: 571–580.
- Vahsen N, Cande C, Briere JJ, Benit P, Joza N, Larochette N *et al.* (2004). AIF deficiency compromises oxidative phosphorylation. *EMBO J* **23**: 4679–4689.
- Yang L, Mashima T, Sato S, Mochizuki M, Sakamoto H, Yamori T *et al.* (2003). Predominant suppression of apoptosome by inhibitor of apoptosis protein in non-small cell lung cancer H460 cells: therapeutic effect of a novel polyarginine-conjugated Smac peptide. *Cancer Res* **63**: 831–837.
- Zamzami N, Marchetti P, Castedo M, Decaudin D, Macho A, Hirsch T *et al.* (1995). Sequential reduction of mitochondrial transmembrane potential and generation of reactive oxygen species in early programmed cell death. *J Exp Med* **182**: 367–377.
- Zhivotovsky B, Orrenius S. (2003). Defects in the apoptotic machinery of cancer cells: role in drug resistance. *Semin Cancer Biol* **13**: 125–134.